Supplementary Information

Porous Zero-Mode Waveguides for Picogram-Level DNA Capture

Vivek Jadhav[†], David P. Hoogerheide[§], Jonas Korlach[#], Meni Wanunu[†,‡,*]

[†]Departments of Physics, Northeastern University, Boston, Massachusetts 02115, USA,

[§]Center for Neutron Research, National Institute of Standards and Technology, Gaithersburg, MD, USA

[#]Pacific Biosciences, Menlo Park, California 94025, USA.

[‡]Departments of Chemistry and Chemical Biology, Northeastern University, Boston, Massachusetts 02115, USA.

*Corresponding author

Email: wanunu@northeastern.edu

Table of Contents

Fabrication of Porous Zero-mode Waveguides (PZMWs)

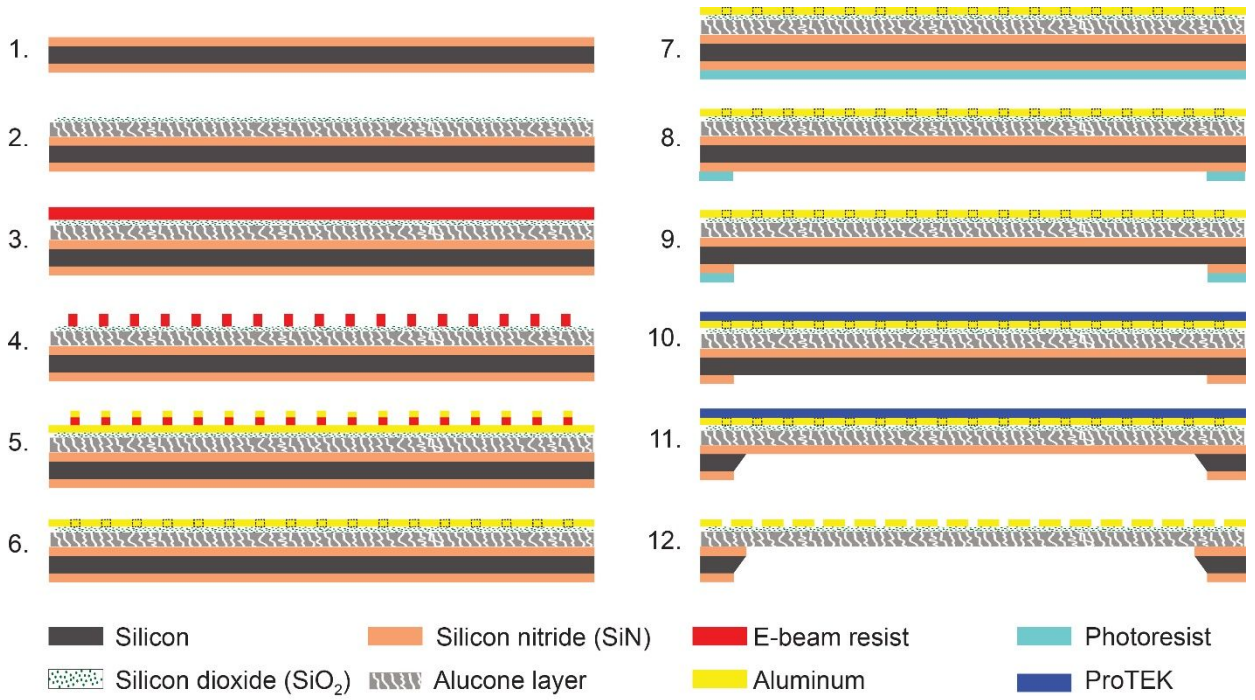

Supplementary Figure 1: Stepwise schematic representation of the PZMW fabrication process: 1. LPCVD SiN-coated silicon wafer (50-nm-thick SiN, 200-µm-thick wafer). 2. ALD deposition of an alucone layer on the SiN membrane, followed by 2-nm-thick SiO_2. 3. Spin-coating of negative e-beam resist (AR-N 7520.11). 4. Electron-beam lithography (EBL) and MF321 development. 5. Thermal evaporation of 100-nm-thick aluminum. 6. Liftoff of resist using 1165 stripper. 7. Positive photoresist (S1818) coating on reverse side of the wafer. 8. Exposure and development of positive photoresist to define etch regions for membranes. 9. Etching of SiN windows using reactive ion etching (RIE). 10. ProTEK spinning and baking to protect aluminum face. 11. Silicon KOH-etching. 12. ProTEK removal using 5-Methyl-2-hexanone and 1-Methyl-2-pyrrolidone.

To fabricate PZMWs we used 200-µm-thick, 4” <100> prime Si wafers. The wafers were RCA cleaned, rinsed with DI H_2O and dried with nitrogen gun. Prior to fabrication, 50 nm of low stress SiN was deposited on either side of the wafer using low pressure chemical vapor deposition (LPCVD) (Fig S1, Step 1). Alucone layer was deposited using trimethylaluminum (TMA) and ethylene glycol (EG) as precursors followed by 2 nm SiO_2 using ALD with Bis(diethylamino)silane (BDEAS) as a precursor and ozone as an oxidizer (Fig S1, Step 2). Alucone coated SiO_2 side of the wafer was used to fabricate ZMWs, which was etched from the reverse side using RIE after KOH.

ZMWs were fabricated using e-beam lithography (EBL) using negative resist (AR-N 7520.11). E-beam resist was spun onto one side of the wafer at 3300 rpm for 45 sec and baked at 90 °C for 60 sec (Fig S1, Step 3). Using a e-beam writer (JEOL 6300FS), a ZMW pattern and alignment mark was exposed in the resist. Alignment marks were used to make sure that the ZMW arrays lined up with photolithography mask to etch down SiN membranes. After exposure, the wafer was developed (MF321 solution) for 90 sec, rinsed with DIH_2O (120 sec) and dried using nitrogen gun. The wafers were descummed in downstream oxygen plasma at 100 watts for 60 sec (Fig S1, Step 4) and 100 nm of aluminum was deposited immediately using thermal evaporator (Fig S1, Step 5). To form metallic ZMWs, overnight lift-off process was done using 1165 stripper solution to ensure complete lift-off (Fig S1, Step 6). To verify proper metallization and lift-off, ZMW patterns were checked with a scanning electron microscope (SEM) prior to photolithography on the back side of the wafer. Positive photoresist (Shipley Microposit S1818) was spun at 4500 rpm for 60 sec on the back side of the wafer and baked at 115 °C for 60 sec (Fig S1, Step 7). The resist was later exposed using a contact aligner (MA/BA 6, Suss MicroTech). A defined pattern was written on the back side of the wafer and was treated using RIE (SF6 plasma) for KOH etching of silicon down to free-standing SiN membrane (Fig S1, Step 8, 9).

ProTEK (Brewer Science) was used to protect the ZMW membranes (Fig S1, Step 10), prior to KOH etch. Silicon was etched using KOH and proTEK was later removed using solvents (Fig S1, Step 11). The backside of the ZMW was completely etched using SF6 plasma (Fig S1, Step 12) giving access to the alucone layer. Prior to the experiment, the chips were immersed in water to form a porous structure.

YOYO-DNA flourescence traces

Here we show 168 PZMWs fluorescence traces from YOYO-1 labelled DNA experiment as discussed in Figure 4e of the main text.

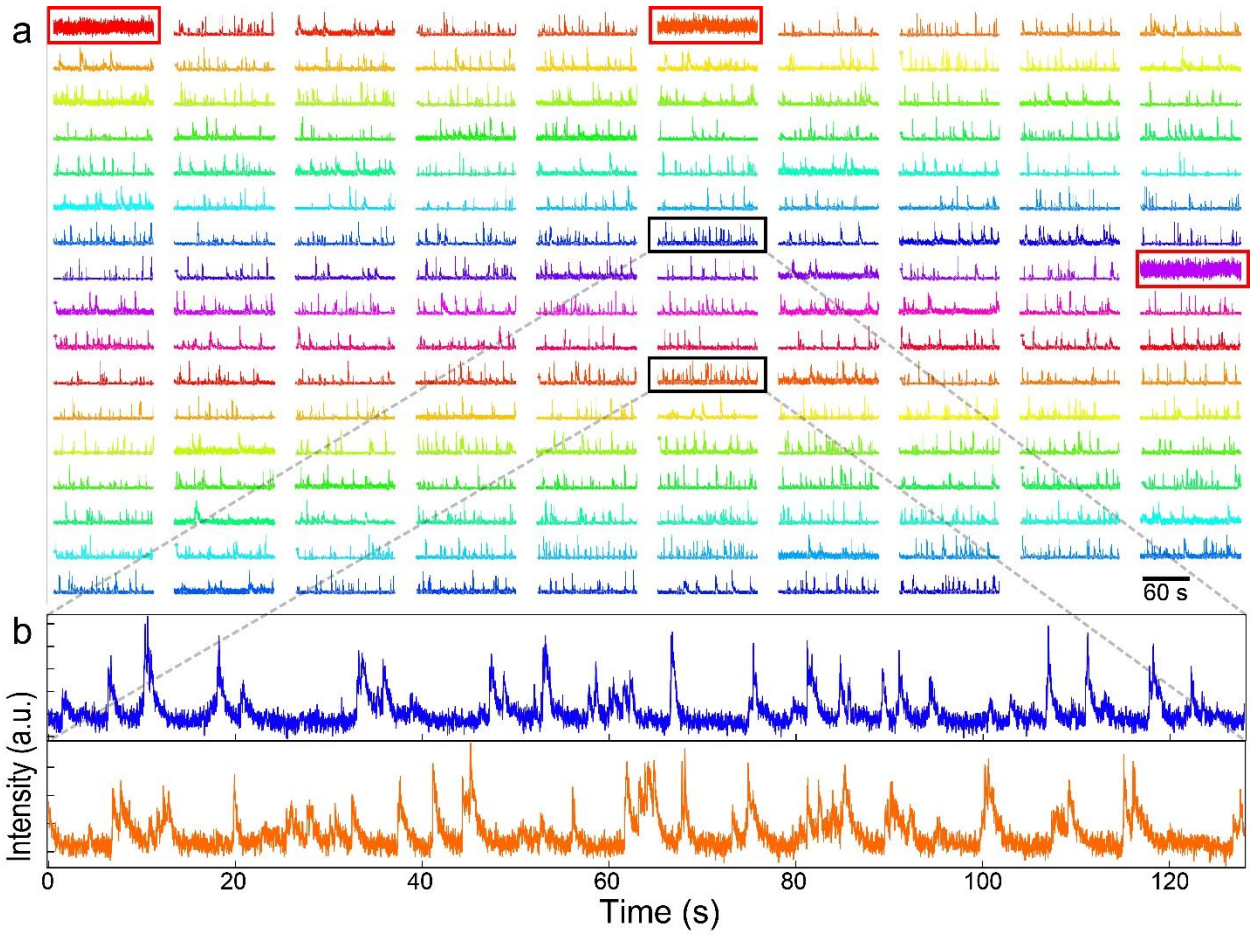

Supplementary Figure 2. DNA capture using PZMWs. a. Fluorescence intensity as a function of time traces from YOYO-DNA in 21x8 PZMWs array at 70 mV voltage bias. DNAs are captured almost in all PZMWs, with the exception of a few due to possible lift-off issues in the fabrication steps, or the lack of a porous structure (faulty PZMWs are highlighted by red rectangles). b. Enlarged traces of DNA capture in two PZMWs as indicated by black rectangle in Fig S2a.

Analysis of captured fluorescence data

Data presented in Figure 4h of the main text were obtained by extracting the fluorescence traces from each PZMW using ImageJ. The fluorescence burst from each YOYO-1 tagged dsDNA was measured (Figure S3). Using Pythion software, each event within the captured frames was analyzed and inter-event time of each peak was determined. One event is considered from the time the DNA enter ZMW until it photobleaches or escapes by diffusion.

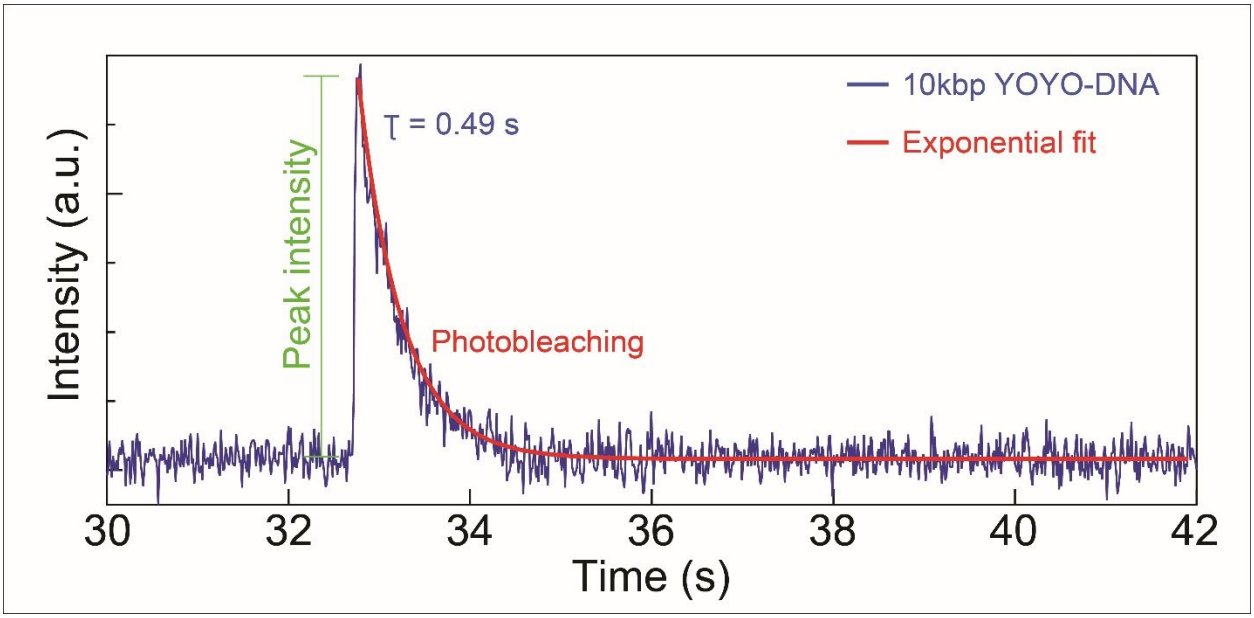

Supplementary Figure 3. PL intensity as a function of time shows 10 kb YOYO-DNA capture, wherein fast rise indicated peak intensity and slow decay suggested photobleaching event in a PZMW.

Electrokinetic capture of biomolecules

The application of PZMW devices are not restricted to capturing of DNA molecules or fluorescently tagged nucleotides; they can also be used to capture other molecules such as ribosome and/or rRNA. Here, we show two capture experiments using fluorescently tagged ribosome [Cy3(L11)70s] and SYBR green II tagged ribosomal RNA.

A ribosome tagged with Cyanine3 (Cy3) fluorescent dye that can be excited using a green laser was used for optical detection using PZMW. We used TAM15 buffer (15 mM MgAc2, 50 mM Tris·HCl, pH 7.5, 30 mM NH_4Cl, 70 mM KCl, and 1 mM DTT) and 10 pM concentration of ribosome for this study. In Figure S4, we have plotted the extracted captured traces of ribosome into PZMW at 200 mV bias. We also used ribosomal RNA (rRNA at 1 pM concentration) from the 70S ribosome of E. coli and fluorescently label them using SYBR Green II using standard protocol (ThermoFisher) for optical detection using PZMW and applying 200 mV voltage bias.

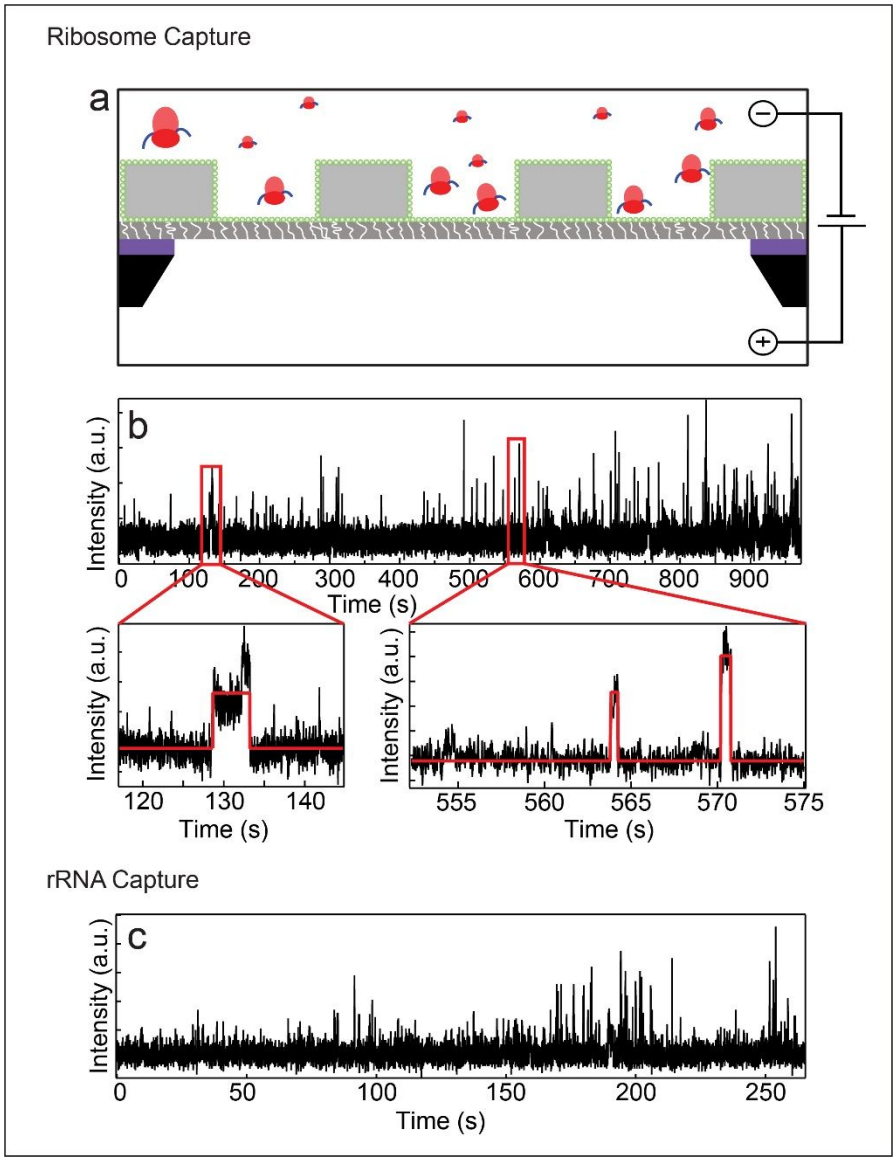

Supplementary Figure 4. Capturing biomolecules using PZMWs. a. Electrophoretic capture of ribosome [Cy3(L11)70s] into PZMWs using 200 mV voltage bias. b. Fluorescence burst from the tagged ribosome excited using green laser, produced a spike during capture at PZMWs (see SI Movie 1), recorded using an emCCD camera and 60X water immersion objective. Bottom two panels show peak intensity as the difference between average baseline fluorescence and peak level. Red line shows each event as computed using Pythion software (https://github.com/rhenley/Pyth-Ion) for dwell time and peak intensity. c. rRNA molecules labeled with SYBR Green II produce fluorescent spikes when they enter and excited using excitation laser within PZMWs. The fluorescence trace is from an individual PZMW at 200 mV voltage bias.

Comparison of loading rates into NZMWs and PZMWs

In Table 1, we present the capture data for long DNA fragments and ribosomal RNA using PZMW (at 0.2 V) compared with our previous NZMW results[1] (at 0.5 V). Indicated concentrations of DNA (pg/µl) were used, and a low voltage bias was applied to the PZMW, which resulted in orders of magnitude enhanced loading rates as compared to NZMW which required sub-nanogram DNA input quantity. We normalized the nucleic acid mass per 1 µl volume and presented that in units of pg^{-1} min^{-1}.

Table S1. Loading rates (#NZMW, %PZMW) ZMW ~ 100 nm,

#*V* = 0.5V.

Analyte (Conc.) *(pg/µl)*	**Rate** *(min^{-1})*	**Loading Rate*** *($pg^{-1}min^{-1}$)*
#λ-DNA, 48-kbp (160)	18	0.12
#*E coli* rRNA, 16+23S (100)	36	0.36
%*V* = 0.2V		
%λ-DNA, 48-kbp (3.2)	67	20.9
%*E coli* rRNA, 16+23s (0.99)	25	25.25

*1 µl sample loading volumes.

Table S1 Comparison of NZMW and PZMW capture data for long fragments of DNA molecules and prokaryotic ribosomal RNA (rRNA) at indicated voltages.

Surface functionalization with Silane Chemistry

For SMRT sequencing, surface functionalization is a critical step. To show that the alucone layer capped with SiO_2 can be functionalized to bind the streptavidin (Stv)-polymerase bound DNA template at the bottom of the PZMWs, we deposited 2 nm SiO_2 atop of a 20-nm-thick MLD alucone layer on a thin microscope cover glass (Fisherbrand – 12-544G) after plasma treatment and a water wash, followed by drying on a hotplate. The cover glass was later passivated using silane-PEG-Biotin for 1hour, after which

excess silane was washed using DI water. The low concentration (200 nM) of Stv conjugated Alexa-647 was added and incubated on the passivated surface of the cover glass and room temperature, the excess Stv-Alexa-647 was washed out using DI water. The cover glass was then mounted on a Total internal reflection fluorescence microscope (TIRF) equipped with EMCCD camera (Andor IXON ultra) and red excitation laser. The immobilized Stv-Alexa-647 by biotin-Stv binding was then excited using a red laser, and the fluorescence was measured overtime. As a measure of control, we repeated the same experiment on a bare cover glass without alucone and SiO2 deposition and measured the excitation.

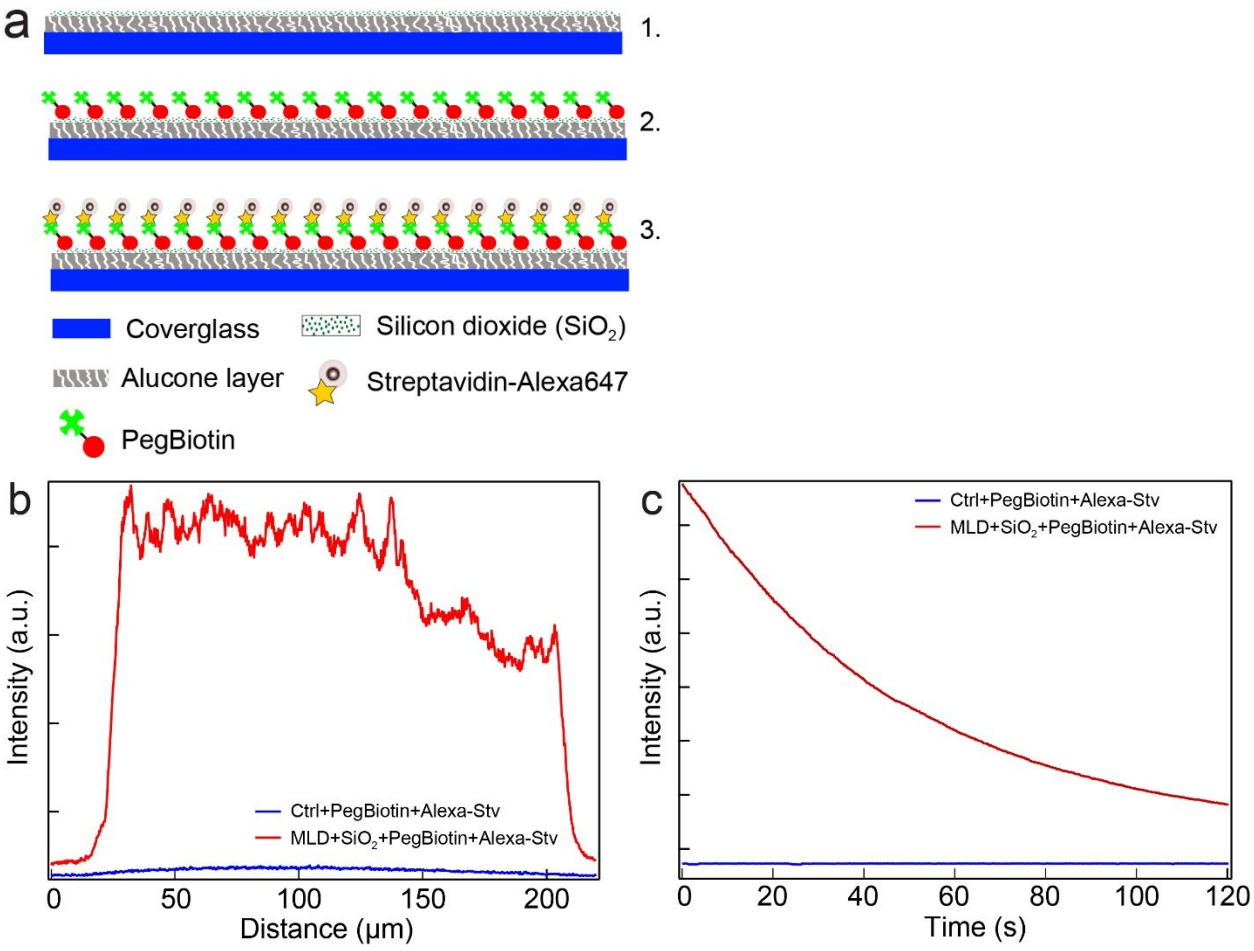

Supplementary Figure 5. Silane binding chemistry on SiO_2 coated alucone surface. a) Schematic representation of surface chemistry, where SiO_2 is coated on top of Alucone layer on a cover glass (a1). Silane-PEG-Biotin is incubated on cover glass at room temperature (a2) and washed using DI water. Stv-Alexa-647 is added on top of the coated cover glass, incubated at room temperature, and washed using DI

water (a3)/ b) The fluorescence from Stv-Alexa-647 when excited using red laser (red curve), confirming the surface functionalization. Blue curve shows no such fluorescence from Stv-Alexa-647, confirming no active binding site at the surface. c) Photobleaching of Stv-Alexa-647 as a function of time (red curve), blue trace does not show any such activity.

References:

(1) Larkin, J.; Henley, R. Y.; Jadhav, V.; Korlach, J.; Wanunu, M. Nat Nanotechnol ***2017,*** *12, 1169-1175.*